Journal of
Applied and Computational Mechanics

Research Paper

Comparison of Functionally Graded Hip Stem Implants with Various Second-Generation Titanium Alloys

Tawakol A. Enab[1], Noha Fouda[2], Ibrahim Eldesouky[3]

[1] Production Engineering and Mechanical Design Department, Faculty of Engineering, Mansoura University, P.O. 35516 Mansoura, Egypt, Email: tenab@mans.edu.eg

[2] Production Engineering and Mechanical Design Department, Faculty of Engineering, Mansoura University, P.O. 35516 Mansoura, Egypt, Email: nfouda@mans.edu.eg

[3] Production Engineering and Mechanical Design Department, Faculty of Engineering, Mansoura University, P.O. 35516 Mansoura, Egypt, Email: ibrahim.eldesouky@mans.edu.eg

Abstract. Total hip Arthroplasty (THA) is performed every year at a very high frequency to improve the quality of life of thousands of patients all over the globe. Nevertheless, the expected service life of such surgery remains unsuitable for patients under 50 years old. This is mainly related to stress shielding and the potential adverse tissue reaction to some of the elements of the market-dominant implant materials. In this research, functionally graded (FG) implant designs of several titanium alloys layered with hydroxyapatite (HA) are proposed to provide lower implant stiffness compared to a solid stem to approach the requirements of human bone. Moreover, TNZT (Ti35Nb7Zr5Ta), and TMZF (Ti12Mo6Zr2Fe) second-generation titanium alloys are studied as a replacement for the famous Ti6Al4V alloy to avoid the adverse tissue reactions related to aluminum and vanadium elements. The different FG models are numerically tested using a 3D finite element simulation after virtual implantation in a femur bone under the dynamic load of a patient descending stairs. In the numerical study, the variation in stress distribution and strain energy in a femur bone is assessed for different FG hip stems as well as the axial stiffness of the hip stems. Results indicated an increase in strain energy and von Mises stress in the cortical and cancellous bones using FG hip stems. Additionally, the axial stiffness is reduced for all FG hip stems relative to the commercial Ti6Al4V hip stem.

Keywords: Functionally graded material (FGM); Second generation titanium alloys; Hip stem implant; Stress shielding; Strain energy.

1. Introduction

β-type titanium alloys (also known as second-generation titanium alloys) are composed of biocompatible elements. They were developed as a possible solution to minimize the stress shielding problem related to the high Young's moduli of current implant materials. Second generation titanium alloys have a Young's modulus closer to the modulus of the bone. Advantages of β-type titanium alloys include lower Young`s moduli, better resistance to corrosion, and improved biocompatibility compared to the famous Ti-6Al-4V alloy [1]. The novel biomedical alloys such as Ti-35Nb-7Zr-5Ta (TNZT) (55GPa) and Ti-12Mo-6Zr-2Fe (TMZF) (80GPa), have low Young's moduli, sufficient strength, and include alloying elements that are completely biocompatible [2, 3]. Studies have been conducted on the implantation of intramedullary rods [4] and bone plates [5] made of TNZT β-type Ti alloys and stainless steel into fractured rabbits tibia. The implantation of both bone plates and intramedullary rods was reported to improve bone remodeling and bone atrophy for TNZT. Results also demonstrated an increase in the diameter of the tibia and the double-wall structure of intramedullary bone for TNZT implants.

Functionally graded materials (FGMs) are special materials whose microstructure or composition, and consequently, the related properties vary according to an assigned law. FGMs captured the scientific community attention due to their broad range of applications. Therefore, intensive researches focused on FGMs fabrication, strength, mechanical, thermal, and vibrational properties [6-16]. Biomedically, FGMs can be adapted to replicate the properties of bone, which minimize the stress shielding effect. Such favorable effects may lead to an increase in the life expectancy of the prostheses. Hedia and Fouda [17] studied the effect of changing Young's modulus of the FG hip stem coating along the vertical direction. Additional study was carried out by Fouda [18] to grade Young`s modulus along the horizontal direction. Both studies showed an increase in the maximum von Mises stress in the surrounding bone at the proximal medial region of the femur while the shear stress was reduced. Darwish et al. [19] compared the fatigue behavior of carbon/PEEK versus PEEK coated hip implant under different human activities.

Additionally, Enab [20] investigated the performance of cemented FGM-coated and uncoated femoral implants with different geometrical models using 2D FE analysis. Moreover, Hedia et al. [21] extended their studies to FGM cemented femoral stem which gives promising results compared to a conventional titanium stem. Besides studying the effect of using FGMs; Al-Jassir et al. [22] examined the effect of changing stem length for functionally graded and conventional implants. They found that the shear stress at bone cement decreased with the stem length while the von Mises stress increased. Gong et al. [23] developed a FE model to

incorporate quantitative functional adaptation theory for the bone with FEA. They observed that the FGM stems have less bone loss compared to titanium stem. FGM1 (titanium at the top HA/Colagen at the bottom) and FGM2 (titanium and bioglass) caused less bone loss compared to titanium stem. The same results were obtained by Hedia et al. [24] using the same bioactive materials to develop the cementless metal backed acetabular cup. A comparison of various FGM femoral prostheses was studied by Oshkour et al. [25]; they concluded that stresses and stress shielding could be adjusted by changing the stiffness of FGM prostheses by managing the volume fraction gradient index. Bahraminasab et al. [26] found that the composition of the implant component`s material must be selected relative to the geometrical design of the component`s. For example, they concluded that 60% porous titanium conical pegs were the optimum solution if they were used with a FGM femoral component; however cylindrical pegs would be preferable in case of using the conventional Co-Cr femoral components. Hedia and Fouda [27] have implemented a 2D axisymmetric FE model of the tibia prosthesis; they observed that the optimal design is to grade the tibia composition vertically. This confirmed the results concluded by Enab [28] and Enab and Bondok [29] when they employed 2D FE models to study the interface stresses for different graded and conventional tibial prostheses. Moreover, Enab [30] proved that it's preferred to design the tibia prosthesis as bidirectional FGMs compared to unidirectional ones. Eldesouky et al. [31] analyzed the performance of low-stiffness hip implants made of second-generation titanium alloys compared to the standard Ti6Al4V implant. Results showed that the bone stresses in the medial and posterior sides of the femur bone increased compared to the reference Ti6Al4V model.

In the current research the concept of using FGMs using the second generation of Ti alloys TNZT and TMZF will be studied using a 3D FE model. A comparison between 6 models will be carried out: a Ti6Al4V stem, a TNZT stem, a TMZF stem, a Ti6Al4V/HA graded stem, a TNZT/HA graded stem and a TMZF/HA graded stem.

2. Materials and Methods

A 3D finite element model was prepared using software (Ansys 17, Pittsburgh, PA, USA) to assess the behavior of cementless hip implants made of different materials. The materials are either a titanium alloy or a longitudinal functionally graded material composed of titanium alloy and hydroxyapatite. The modulus of elasticity of the functionally graded implants was graded along a direction from the proximal end to the distal end in the sagittal plane. A 3D model of a commercial femur bone (Third gen. femur, Pacific Research Labs, WA, USA) was utilized to represent the bone [32]. The design of the hip stem was modified from previously published research [33, 34]. Dimensions of the studied hip stem design are shown in Fig. 1. The implant was designed using a computer aided design package (SolidWorks 2017, Dassault Systèmes, Waltham, MA, USA). The assembly model of the implant within the femur bone was modelled using the same software. The CAD assembly file was imported in Ansys Workbench for preparing the mesh, defining contact, and setting the boundary conditions. Next, the model was exported to Ansys APDL for incorporating the functionally graded material model. The assembly model was evaluated using the dynamic force measured experimentally in literature for a patient descending stairs [35, 36] as shown in Fig. 2. The loading cycle was modelled as ten consecutive load steps varying with time. An additional force (F2) of 1265N was applied to the bone to compensate for the abductor muscle pulling force [37]. The femur bone was assumed to be fixed at the distal end (Fig. 3).

The assembly model consisted of four parts (cortical bone, cancellous bone, top neck implant section, proximal and distal implant end). Classifying the CAD model as four parts was essential to assign different material properties for each part. The cortical and cancellous bones were assumed to have orthotropic, homogeneous material properties. Bone properties listed in Table 1 were taken from previous literature [38-40]. A total of six finite element models were simulated. In three models the entire hip stem was modelled as one of the titanium alloys Ti6Al4V, Ti35Nb5Ta7Zr (TNZT), or Ti12Mo6Zr2Fe (TMZF). The remaining three models had a one of titanium alloys neck and a functionally graded distal end. Table 2 presents the classification of materials used for neck and distal sections of the implanted stems for the different models. The properties of titanium alloys are illustrated in Table 3 [41, 42]. The mechanical properties of the distal section of the hip stem were graded starting with the titanium alloy at the proximal and ending with hydroxyapatite at the distal.
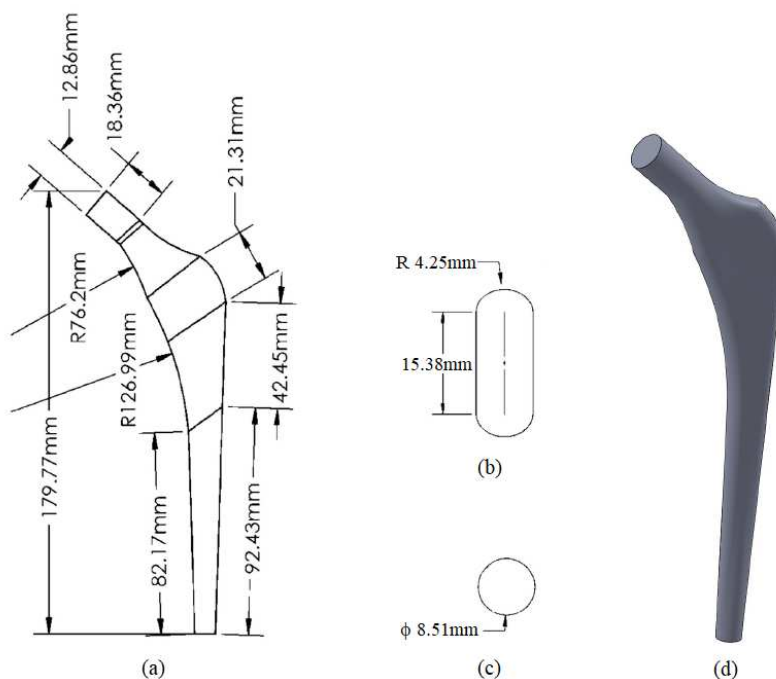

Fig. 1. Femoral hip stem design (a) 2D profile, (b) Proximal cross section, (c) distal cross section (a, b, c after [33, 34]), and (d) 3D profile.

Table 1. Bone properties employed in the finite element model [38-40].

Material	Modulus of Elasticity (MPa)	Shear modulus (GPa)	Poisson's ratio	Compressive Strength (MPa)	Density g/cm³
Cortical bone	$E_x = 6979$	$G_{yz} = 5.6$	$v_{yz} = 0.25$	195	2.02
	$E_y = 18132$	$G_{zx} = 4.5$	$v_{zx} = 0.4$		
	$E_z = 6979$	$G_{xy} = 6.2$	$v_{xy} = 0.25$		
Cancellous bone	$E_x = 660$	$G_{yz} = 0.211$	$v_{yz} = 0.25$	16	1.37
	$E_y = 1740$	$G_{zx} = 0.165$	$v_{zx} = 0.4$		
	$E_z = 660$	$G_{xy} = 0.260$	$v_{xy} = 0.25$		

Table 2. Materials used for neck and distal sections of stem.

Model No.	Material of the neck section	Material of the distal section
1	Ti6Al4V	Ti6Al4V
2	Ti12Mo6Zr2Fe (TMZF)	Ti12Mo6Zr2Fe (TMZF)
3	Ti35Nb7Zr5Ta (TNZT)	Ti35Nb7Zr5Ta (TNZT)
4	Ti6Al4V	FGM starting with Ti6Al4V at the top and ending with HA at the bottom
5	Ti12Mo6Zr2Fe (TMZF)	FGM starting with (TMZF) at the top and ending with HA at the bottom
6	Ti35Nb7Zr5Ta (TNZT)	FGM starting with (TNZT) at the top and ending with HA at the bottom

Table 3. Properties of the materials under study [41, 42].

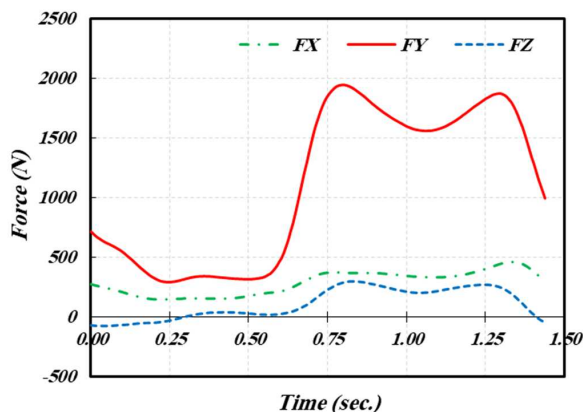| Material	Ti6Al4V	TNZT (Ti35Nb5Ta7Zr)	TMZF (Ti12Mo6Zr2Fe)	Hydroxyapatite
ASTM	F136	-	F1813	F1185
Density (g/cm³)	4.42	5.72	4.89	3.15
Modulus of elasticity (GPa)	120	55	74-85	7-13
Yield strength (MPa)	930	547	1000	-
Ultimate compressive strength (MPa)	970	597	1060	350-450

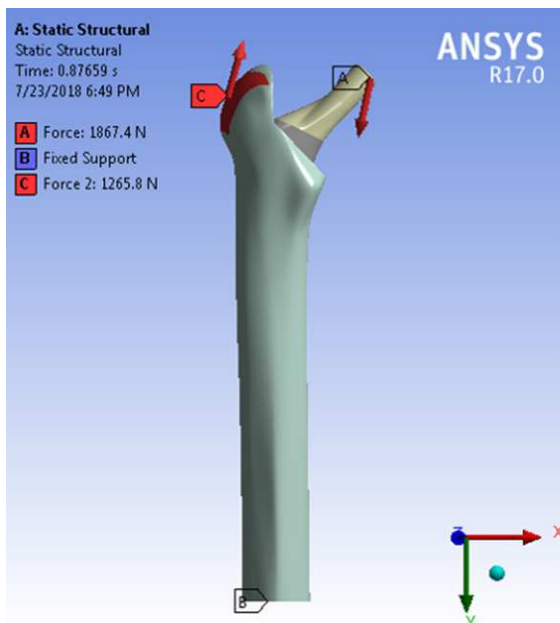**Fig. 2.** Forces applied on the finite element model.

Fig. 3. The Directions of applied loads and the position of fixation modeled in the numerical study.

The bone-stem assembly was tessellated to approximately 86347 tetrahedral (Tet10) elements with an element size of 2 mm. The element size was selected based on a mesh convergence study that demonstrated negligible variation in the results when a smaller element size was used. The mesh quality was evaluated using different criteria of which the orthogonal quality for the mesh was 0.76, while the skewness was 0.39, demonstrating that the geometric model was represented accurately. The neck, and the distal parts of the hip stem implant were bonded despite their different material properties to represent a single part. Contact conditions between the hip implant and each of the cancellous and cortical bones were modelled as frictional contact with a coefficient of 0.4 as measured experimentally in literature [43]. The frictional nonbonded condition represents the situation immediately after surgery and before bone ingrowth.

The functionally graded hip stem implant models composed of Ti alloy–HA. The variation in the elastic modulus (E) of the implant in the longitudinal direction can be expressed as:

$$E = \frac{E_O(1-p)}{1+\left[(p(5+8\nu)(37-8\nu))/(8(1+\nu)(23+8\nu))\right]} \tag{1}$$

where:

$$E_O = E_2\left[\frac{E_2+(E_1-E_2)V_1^{2/3}}{E_2+(E_1-E_2)(V_1^{2/3}-V_1)}\right] \tag{2}$$

$$\nu = \nu_1 V_1 + \nu_2 V_2 \tag{3}$$

where p is the FGM porosity, E_0 denotes the Young's modulus for fully dense material, ν_1, ν_2, E_1, E_2 and V_1, V_2 are Poisson's ratios, elastic moduli and the volume fractions of the two materials, respectively [13, 17, 20].

3. Results and Discussion

Finite element modelling is considered as a promising and effective tool in the assessment of bone implants to establish a good clinical practice. The numerical models built in the current study were developed to best represent the implanted human hip joint, as well as to predict the stresses distribution using different implant materials.

Finite element analysis (FEA) offers a major advantage that it can be used to calculate stresses throughout the entire bone and implant assembly. Therefore, a comparison of stress distribution in a femur bone implanted with six hip stem implants with different materials was possible. The von Mises stresses in the cancellous bone remained almost the same for the first four load steps of the load cycle for all hip stem materials. A maximum von Mises bone stress was recorded at the distal end where the model was fixed and the displacement of the same surface was zero verifying that the model meets the specifications. The maximum implant von Mises stress was 110 MPa in the solid neck section. The value and location of the maximum implant stress are in agreement with the previously published results [44-47].

The result indicated an increase in von Mises stresses in the cancellous bone in load steps from 5 to 10 as illustrated in Fig. 4. The von Mises stress increased when the commonly used Ti6Al4V alloy was replaced by the second-generation titanium alloys or their functionally graded counterparts. The maximum increase was recorded in model number 6 (TNZT) as described in Table 2 in which the stress reached double the values of Ti6Al4V.

A percentage difference of von Mises stress for stem models (2-6) relative to Ti6Al4V stem (model 1) at load step 9 was illustrated in Fig. 5 (a and b). This percentage was presented for cortical and cancellous bone. It was observed from both Figs. that the percentage of von Mises stress in cancellous and cortical bone increased using all FGM stems compared to Ti alloy stems. As well as, the percentage increase of von Mises stress is higher in cancellous bone than cortical bone for all stem models. As shown in Fig. 5-a, in cancellous bone von Mises stress percentage was increased by 102%, 81% and 66% for (TNZT-HA), (TMZF-HA) and (Ti6Al4V-HA) FGM stems compared to Ti6Al4V stem, respectively. While for TNZT and TMZF, von Mises stress increased by 50% and 22% compared to Ti6Al4V stem, respectively. In cortical bone, Fig. 5-b, the maximum increase in von Mises stress occurred using TNZT-HA stem with a value equals 2% compared to Ti6Al4V stem. Moreover, for TMZF-HA and Ti6Al4V-HA von Mises stress increased by 1.5% and 1% compared to Ti6Al4V stem, respectively.

The variations of the von Mises stress distributions occurring in cortical bone at load step 9 for the different stem materials models are illustrated in figures 6 to 8. It is essential to highlight that; the same range of contour levels and colors was considered for all models to clearly demonstrate the differences in stress levels and distributions. The main point of interest from these figures; (i.e. Figs. 6-8); is the clear difference between the stress distributions and their levels occurring in the cortical bone when using Ti alloys and FGM stems. It is clear that, the use of FGM stems has a great effect on the stress distributions in the medial side of the cortical bone since there is a wide growth in the regions of maximum stresses. Such growth demonstrates that there is an increase in the loading of the cancellous and cortical bones.
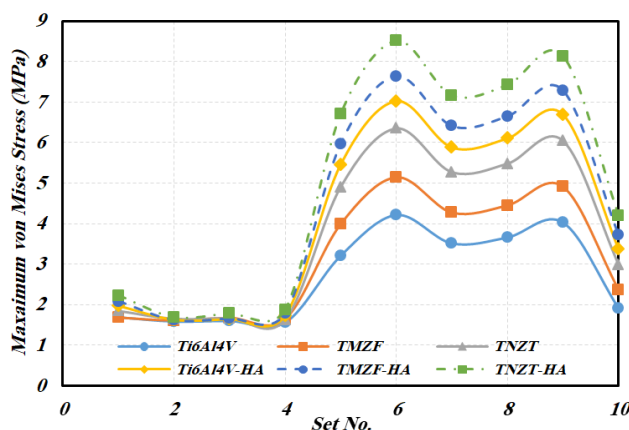

Fig. 4. Variation of maximum von Mises stresses in cancellous bone over the loading cycle for different models.
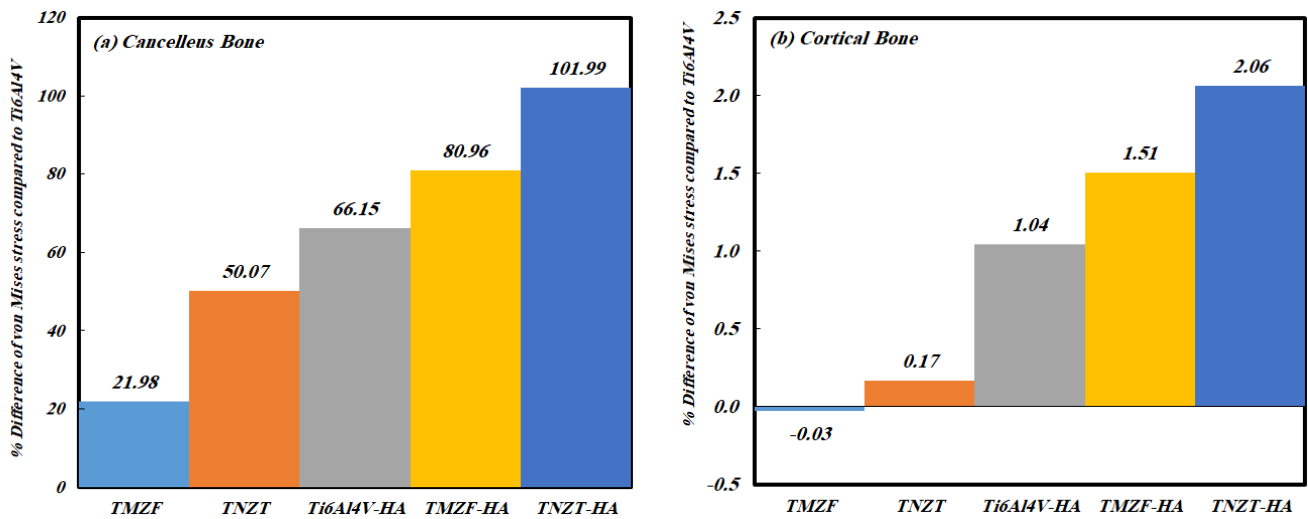
Fig. 5. Percentage difference of maximum von Mises stress for different models compared to Ti6Al4V at load step 9 for (a) cancellous bone and (b) cortical bone.
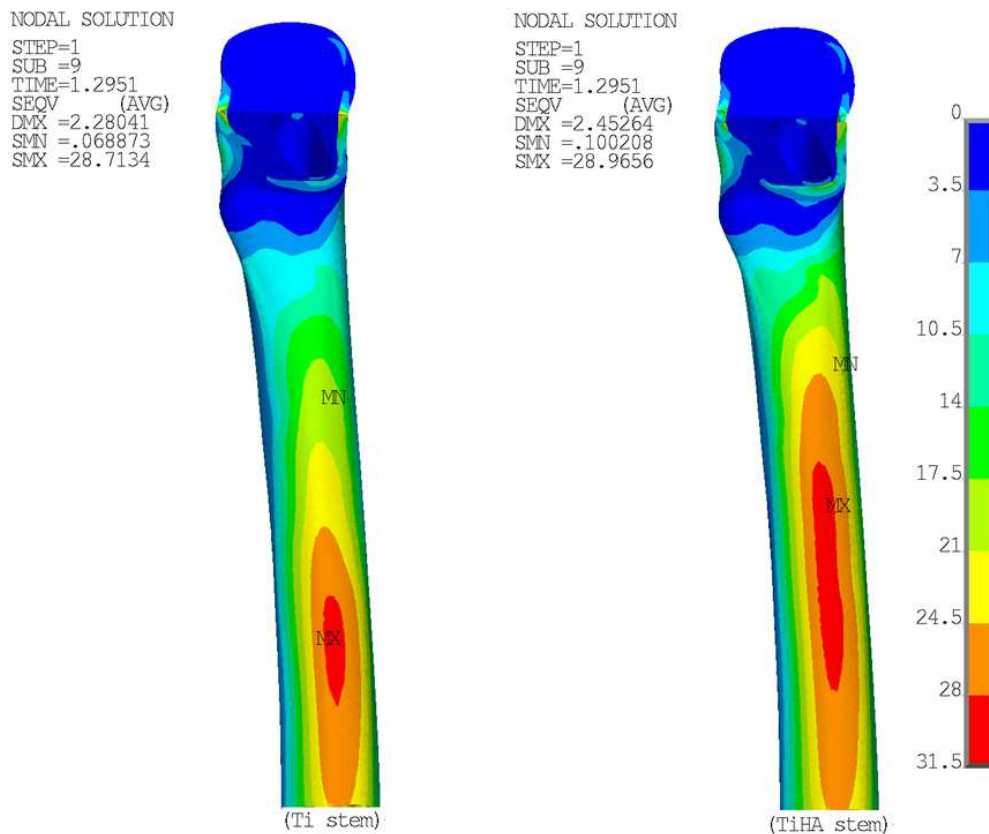

Fig. 6. von Mises stress distribution in cortical bone at load step 9 for Ti6Al4V stem (left) and FGM Ti6Al4V-HA stem (right).

The average strain energy is increased in both cortical and cancellous bone using a femur stem from the second generation Ti alloys as a functionally graded material with HA. The percentage difference of the average strain energy for stem models (from 2 to 6) compared to Ti6Al4V stem (model 1) at the highest applied load (step 9) is illustrated in Fig. 9 (a and b) for both cancellous and cortical bones. The maximum increase was recorded for the TNZT-HA hip stem for both cancellous and cortical bones. This is considered as an indication of the reduction in stress shielding.

The total deformation of the hip stem was calculated in the vertical direction for all material combinations. The applied force at load step 9 was divided by the calculated deformation to obtain the axial stiffness of each implant. The percentage difference of axial stiffness for femoral stem models (2-6) compared to Ti6Al4V stem (model 1) is illustrated in Fig.10. Results showed that the femoral stem axial stiffness decreased for all FGM stems compared to their titanium counterparts. As shown in Fig. 10, the percentage difference of axial stiffness was decreased by 28.5%, 22.5% and 17.8% for (TNZT-HA), (TMZF-HA) and (Ti6Al4V-HA) FGM stems compared to Ti6Al4V stem, respectively. While for TNZT and TMZF, axial stiffness decreased by 20% and 9.9% compared to Ti6Al4V stem, respectively.
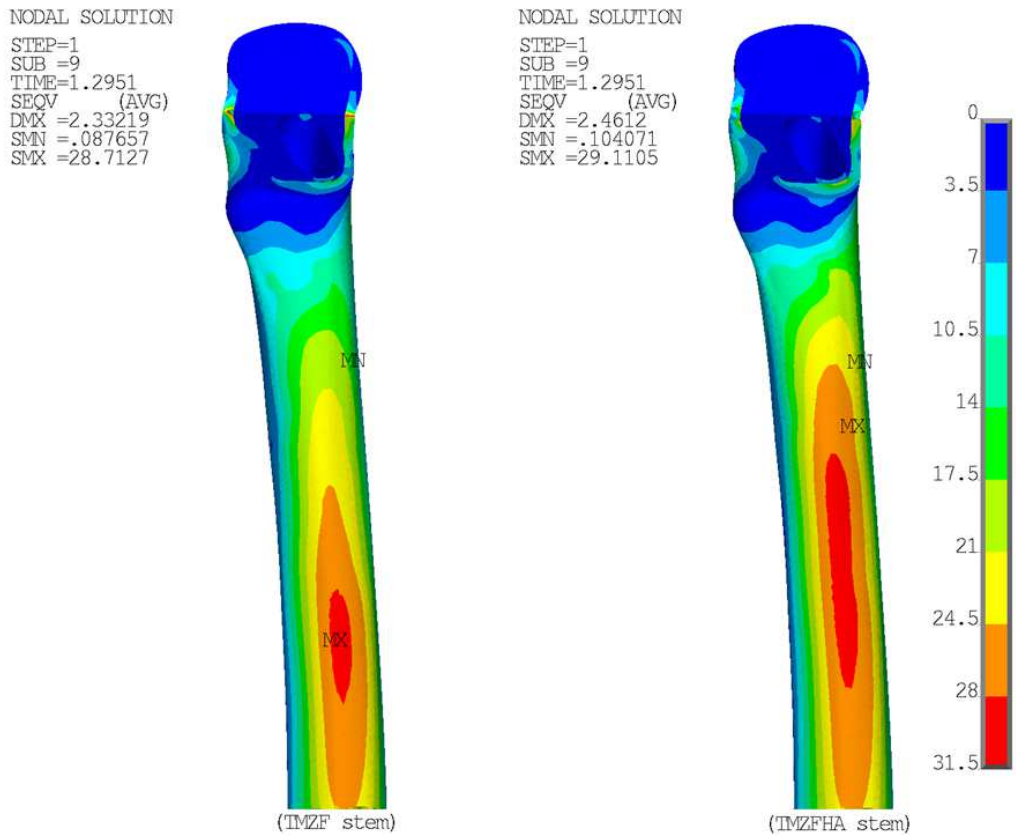
Fig. 7. von Mises stress distribution in cortical bone at load step 9 for TMZF stem (left) and FGM TMZF-HA stem (right).
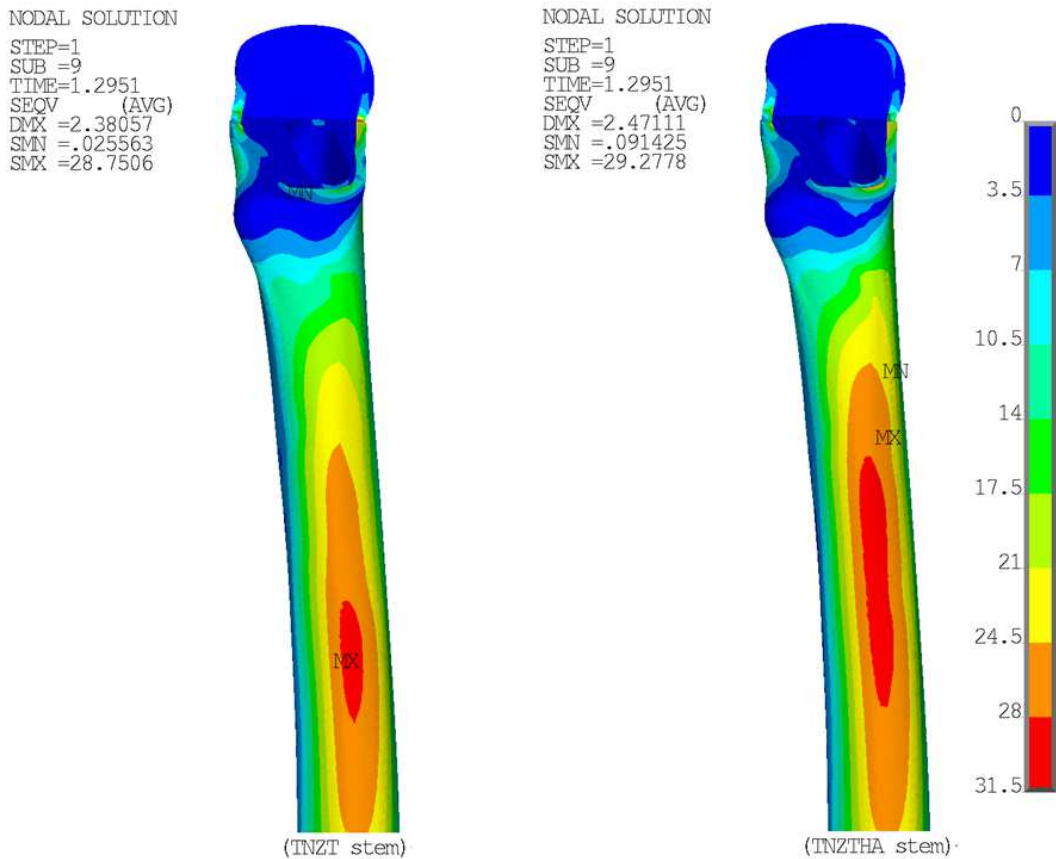

Fig. 8. von Mises stress distribution in cortical bone at load step 9 for TNZT stem (left) and FGM TNZT-HA stem (right).

Therefore, from figures 5 to 10, it can be concluded that decreasing the implant stiffness resulted in more homogeneous stress distribution matching the normal physiological range compared the nongraded implant. This may be explained by that the lower the implant stiffness, the higher the stresses transferred to the bone. The increase in bone stresses reduces stress shielding of the bone, bone loss, and implant loosening.
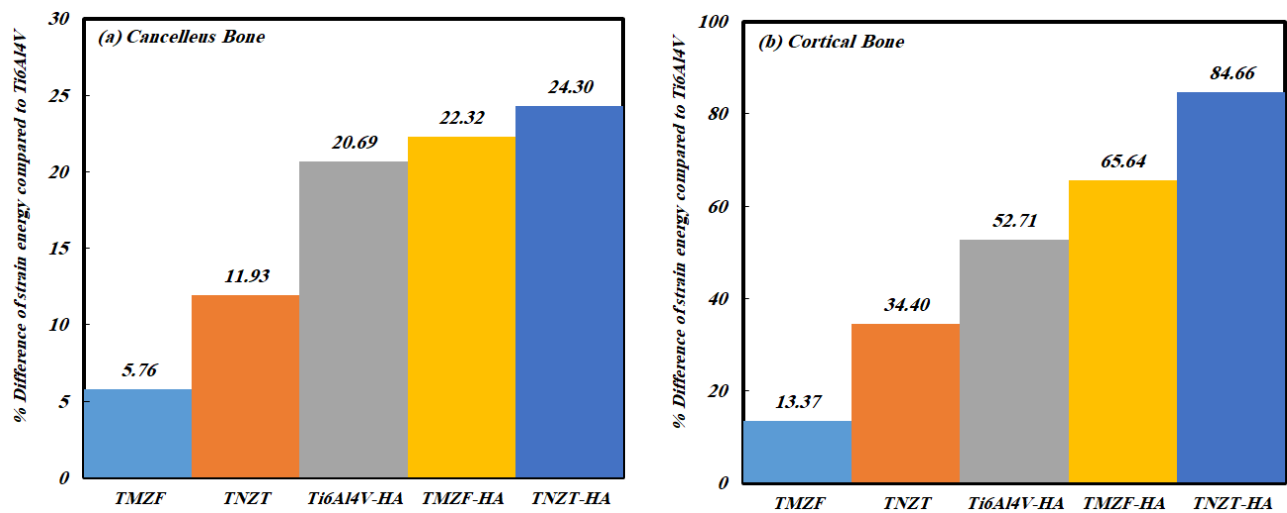
Fig. 9. Percentage difference of strain energy for different models compared to Ti6Al4V at load step 9 for (a) cancellous bone and (b) cortical bone.
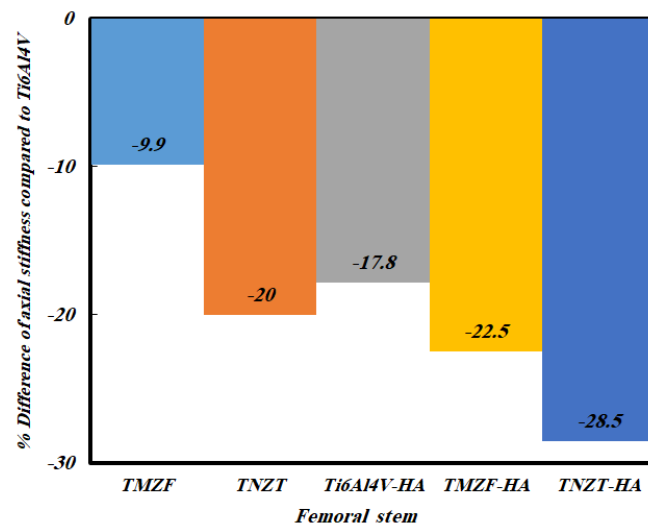

Fig. 10. Percentage difference of axial stiffness for different models compared to Ti6Al4V at load step 9 for femoral stem.

4. Conclusion

In the current research, the performance of functionally graded hip stem implants was compared with second-generation Ti alloys using 3D FE models. A comparison between six different models was carried out. Present study results lead to the following conclusions:

➤ The maximum von Mises stress increased in both cortical and cancellous bone using a functionally graded femoral stem based on the second generation of Ti alloys with HA.
➤ In cortical and cancellous bones, the maximum increase in von Mises stress occurred using the TNZT-HA stem.
➤ All FGM stem models showed that higher stresses were distributed to a larger area of the proximal medial region of the cortical bone compared to Ti alloys stem models.
➤ Average strain energy increased using a femur stem from the second generation of Ti alloys as an FGM with HA in both cortical and cancellous bones.
➤ Axial stiffness decreased for all FGM stems compared to their titanium counterparts.
➤ The increase in strain energy and maximum stresses is considered a reduction in stress shielding and consequently improves the life span of the implant.

Author Contributions

T. A. Enab planned the scheme, initiated the project, and suggested the FEM models; I. Eldesouky developed the CAD model and developed the first Ti-alloy FEM model; T. A. Enab and N. Fouda developed and conducted the functionally graded materials FEM models. All authors examined the validation of the developed FEM models and analyzed the results. The manuscript was written through the contribution of all authors. All authors discussed the results, reviewed and approved the final version of the manuscript.

Conflict of Interest

The authors declared no potential conflicts of interest with respect to the research, authorship and publication of this article.

Funding

References

[1] Niinomi, M., Recent metallic materials for biomedical applications, *Metallurgical and Materials Transactions* A, 33(3), 2002, 477.

[2] Wang, K., The use of titanium for medical applications in the USA, *Materials Science and Engineering: A*, 213(1-2), 1996, 134-137.

[3] Long, M. and H. Rack, Titanium alloys in total joint replacement-a materials science perspective, Biomaterials, 19(18), 1998, 1621-1639.

[4] Yaszemski, M.J., *Biomaterials in orthopedics*, CRC Press, 2003.

[5] Sumitomo, N., et al., Experiment study on fracture fixation with low rigidity titanium alloy, *Journal of Materials Science: Materials in Medicine*, 19(4), 2008, 1581-1586.

[6] Eltaher, M., S.A. Emam, and F. Mahmoud, Free vibration analysis of functionally graded size-dependent nanobeams, *Applied Mathematics and Computation*, 218(14), 2012, 7406-7420.

[7] Enab, T.A., Stress concentration analysis in functionally graded plates with elliptic holes under biaxial loadings, *Ain Shams Engineering Journal*, 5(3), 2014, 839-850.

[8] Sedighi, H.M., M. Keivani, and M. Abadyan, Modified continuum model for stability analysis of asymmetric FGM double-sided NEMS: corrections due to finite conductivity, surface energy and nonlocal effect, *Composites Part B: Engineering*, 83, 2015, 117-133.

[9] Eltaher, M., et al., Modified porosity model in analysis of functionally graded porous nanobeams, *Journal of the Brazilian Society of Mechanical Sciences and Engineering*, 40(3), 2018, 141.

[10] Soliman, A.E., et al., Nonlinear transient analysis of FG pipe subjected to internal pressure and unsteady temperature in a natural gas facility, *Structural Engineering and Mechanics*, 66(1), 2018, 85-96.

[11] Akba, .D., Hygro-thermal nonlinear analysis of a functionally graded beam, *Journal of Applied and Computational Mechanics*, 5(2), 2019, 477-485.

[12] Rahmani, M., et al., Vibration analysis of different types of porous FG conical sandwich shells in various thermal surroundings, *Journal of Applied and Computational Mechanics*, 6(3), 2020, 416-432.

[13] Nemat-Alla, M., Reduction of thermal stresses by developing two-dimensional functionally graded materials, *International Journal of Solids and Structures*, 40(26), 2003, 7339-7356.

[14] Park, J., Park, K., Kim, J., Jeong, Y., Kawasaki, A., Kwon, H., Fabrication of a Functionally Graded Copper-Zinc Sulfide Phosphor, *Scientific Reports*, 6(1), 2016, 23064.

[15] Hu, S., Gagnoud, A., Fautrelle, Y., Moreau, R., Li, X., Fabrication of aluminum alloy functionally graded material using directional solidification under an axial static magnetic field, *Scientific Reports*, 8(1), 2018, 7945.

[16] Ghamkhar, M., Naeem, M.N., Imran, M., Kamran, M., Soutis, C., Vibration frequency analysis of three-layered cylinder shaped shell with effect of FGM central layer thickness, *Scientific Reports*, 9(1), 2019, 1566.

[17] Hedia, H., Fouda, N., Design optimization of cementless hip prosthesis coating through functionally graded material, *Computational Materials Science*, 87, 2014, 83-87.

[18] Fouda, N., Horizontal functionally graded material coating of cementless hip prosthesis, *Trends Biomater. Artif. Organs*, 28(2), 2014, 58-64.

[19] Darwich, A., Nazha, H., Daoud, M., Effect of Coating Materials on the Fatigue Behavior of Hip Implants: A Three-dimensional Finite Element Analysis, *Journal of Applied and Computational Mechanics*, 6(2), 2020, 284-295.

[20] Enab, T.A., Behavior of FGM-coated, HA-coated and uncoated femoral prostheses with different geometrical configurations, *International Journal of Mechanical and Mechatronics Engineering IJMME-IJENS*, 16(3), 2016, 62-71.

[21] Hedia, H., Aldousari, S.M., Abdellatif, A.K., Fouda, N., A new design of cemented stem using functionally graded materials (FGM), *Bio-medical Materials and Engineering*, 24(3), 2014, 1575-1588.

[22] Al-Jassir, F.F., Fouad, H., Alothman, O.Y., In vitro assessment of Function Graded (FG) artificial Hip joint stem in terms of bone/cement stresses: 3D Finite Element (FE) study, *Biomedical Engineering Online*, 12(1), 2013, 5.

[23] Gong, H., Kong, L., Zhang, R., Fang, J., Zhao, M., A femur-implant model for the prediction of bone remodeling behavior induced by cementless stem, *Journal of Bionic Engineering*, 10(3), 2013, 350-358.

[24] Hedia, H., El-Midany, T.T., Shabara, M.A.N., Fouda, N., Development of cementless metal-backed acetabular cup prosthesis using functionally graded material, *International Journal of Mechanics and Materials in Design*, 2(3-4), 2005, 259-267.

[25] Oshkour, A.A., Talebi, H., Shirazi, S.F.S., Bayat, M., Yau, Y.H., Tarlochan, F., Abu Osman, N.A., Comparison of various functionally graded femoral prostheses by finite element analysis, *The Scientific World Journal*, 2014, 2014, 1-17.

[26] Bahraminasab, M., Sahari, B.B., Edwards, K.L., Farahmand, F., Jahan, A., Hong, T.S., Arumugam, M., On the influence of shape and material used for the femoral component pegs in knee prostheses for reducing the problem of aseptic loosening, *Materials & Design*, 55, 2014, 416-428.

[27] Hedia, H.S., Fouda, N., Improved stress shielding on a cementless tibia tray using functionally graded material, *Materials Testing*, 55(11-12), 2013, 845-851.

[28] Enab, T.A., A comparative study of the performance of metallic and FGM tibia tray components in total knee replacement joints, *Computational Materials Science*, 53(1), 2012, 94-100.

[29] Enab, T.A., Bondok, N.E., Material selection in the design of the tibia tray component of cemented artificial knee using finite element method, *Materials & Design*, 44, 2013, 454-460.

[30] Enab, T.A., Performance Improvement of Total Knee Replacement Joint through Bidirectional Functionally Graded Material, *International Journal of Mechanical and Mechatronics Engineering IJMME-IJENS*, 14(2), 2014, 104-113.

[31] Eldesouky, I., El-Hofy, H., Harrysson, O., Design and Analysis of a Low-Stiffness Porous Hip Stem, *Biomedical Instrumentation & Technology*, 51(6), 2017, 474-482.

[32] Papini, M., Zalzal, P. , Third generation composite femur. *Biomechanics European Laboratory: The BEL Repository*, 2015.

[33] Oshkour, A., Abu Osman, N.A., Bayat, M., Afshar, R., Berto, F., Three-dimensional finite element analyses of functionally graded femoral prostheses with different geometrical configurations, *Materials & Design*, 56, 2014, 998-1008.

[34] Oshkour, A.A., Talebi, H., Shirazi, S.F.S., Yau, Y.H., Tarlochan, F., Abu Osman, N.A., Effect of Geometrical Parameters on the Performance of Longitudinal Functionally Graded Femoral Prostheses, *Artificial Organs*, 39(2), 2015, 156-164.

[35] Bergmann, G., Deuretzbacher, G., Heller, M., Graichen, F., Rohlmann, A., Strauss, J., Duda, G.N., Hip contact forces and gait patterns from routine activities, *Journal of Biomechanics*, 34(7), 2001, 859-871.

[36] Bergmann, G., Graichen, F., Rohlmann, A., Bender, A., Heinlein, B., Duda, G.N., Heller, M.O., Morlock, M.M., Realistic loads for testing hip implants, *Bio-medical Materials and Engineering*, 20(2), 2010, 65-75.

[37] Pawlikowski, M., Skalski, K., Haraburda, M., Process of hip joint prosthesis design including bone remodeling phenomenon, *Computers & Structures*, 81(8-11), 2003, 887-893.

[38] Kokubo, T., Kim, H.M., Kawashita, M., Novel bioactive materials with different mechanical properties, *Biomaterials*, 24(13), 2003, 2161-2175.

[39] Peng, L., Bai, J., Zeng, X., Zhou, Y., Comparison of isotropic and orthotropic material property assignments on femoral finite element models under two loading conditions, *Medical Engineering & Physics*, 28(3), 2006, 227-233.

[40] Syahrom, A., Januddi, M.A.M.S., Harun, M.N., Öchsner, A., Cancellous Bone: Mechanical Characterization and Finite Element Simulation, Springer, Singapore, Vol. 82, 2017.

[41] Niinomi, M., Mechanical properties of biomedical titanium alloys, *Materials Science and Engineering: A*, 243(1-2), 1998, 231-236.

[42] Pilliar, R.M., Metallic biomaterials, in Biomedical materials, Springer, 2009, 41-81.

[43] Rancourt, D., Shirazi-Adl, A., Drouin, G., Paiement, G., Friction properties of the interface between porous-surfaced metals and tibial cancellous bone, *Journal of Biomedical Materials Research*, 24(11), 1990, 1503-1519.

[44] Bougherara, H., Zdero, R., Shah, S., Miric, M., Papini, M., Zalzal, P., Schemitsch, E.H., A biomechanical assessment of modular and monoblock revision hip implants using FE analysis and strain gage measurements, *Journal of Orthopaedic Surgery and Research*, 5, 2010, 34.

[45] Oshkour, A.A., Abu Osman, N.A., Yau, Y.H., Tarlochan, F., Abas, W.W., Design of new generation femoral prostheses using functionally graded materials: a finite element analysis, *Journal of Engineering in Medicine*, 227(1), 2013, 3-17.

[46] Baharuddin, M.Y., Salleh, S., Zulkifly, A.H., Lee, M.H., Noor, A.M., Harris, A.R.A., Abdul Majid, N., Abd Kader, A.S., Design process of cementless femoral stem using a nonlinear three dimensional finite element analysis, *BMC Musculoskelet Disord*, 15, 2014, 30.

[47] Rezaei, F., Hassani, K., Solhjoei, N., Karimi, A., Carbon/PEEK composite materials as an alternative for stainless steel/titanium hip prosthesis: a finite element study, *Australasian Physical & Engineering Sciences in Medicine*, 38(4), 2015, 569-580.

ORCID iD

Tawakol A. Enab https://orcid.org/0000-0003-1201-6547
Noha Fouda https://orcid.org/0000-0002-1206-7486
Ibrahim Eldesouky https://orcid.org/0000-0003-3926-5471

Publisher's Note Shahid Chamran University of Ahvaz remains neutral with regard to jurisdictional claims in published maps and institutional affiliations.